

# Laser Desorption Jet-Cooling of Organic Molecules

## Cooling Characteristics and Detection Sensitivity

G. Meijer, M. S. de Vries, H. E. Hunziker, and H. R. Wendt

IBM Research Division, Almaden Research Center, 650 Harry Road, San Jose, CA 95120-6099, USA

Received 20 July 1990/Accepted 9 August 1990

**Abstract.** Laser desorption followed by jet-cooling allows wavelength-selective as well as mass-selective detection of molecules desorbed from a surface without fragmentation. The cooling characteristics and detection sensitivity of laser desorption jet-cooling of organic molecules are investigated. From the rotational contour of the electronic origin of the  $S_1 \leftarrow S_0$  transition of laser-desorbed anthracene, rotational cooling to 5–10 K is demonstrated. Vibrational cooling is studied for laser-desorbed diphenylamine, a molecule with low-energy vibrations, and a vibrational temperature below 15 K is found. The absolute detection sensitivity is determined for the perylene molecule. Using two-color (1 + 1) resonance enhanced multi-photon ionization (with a measured ionization efficiency of 0.25) for detection, it is found that one ion is produced in the detection region for every  $2 \times 10^5$  perylene molecules evaporated from the desorption laser spot. A two-color (1 + 1) REMPI spectrum (400 points) of perylene is recorded using only 30 picogram of material.

**PACS:** 35.80 s, 82.80 Bi, 47.45 Nd

In the laser desorption jet-cooling technique, molecules originally adsorbed on a surface are desorbed with a laser pulse close to the orifice of a pulsed jet expansion. The laser-desorbed molecules are entrained in the jet and their internal energy is cooled by multiple collisions in the expansion region. In the collision-free region of the expansion the molecular beam is probed with one or more ionization laser(s), and ions are mass- and wavelength-selectively detected [1–6]. Cooling is important both for simplifying the spectroscopy of the desorbed molecules [7] and for increasing the detection efficiency; one can take advantage of resonance-enhanced multi-photon ionization (REMPI) spectroscopy to achieve sensitive and selective detection [8]. Even when non-resonant ionization techniques are used to detect the entrained molecules, cooling has the advantage that it results in less fragmentation following ionization. When compared with the more commonly used laser desorption technique in which ionization of the desorbates is performed close to the surface, selectivity and ionization efficiency are higher with jet-cooling. The fraction of the desorbed molecules brought into the detection region, however, is expected to be smaller for the latter technique [9].

In this report our laser desorption jet-cooling apparatus is described in detail. Measurements are presented

from which the degree of both rotational and vibrational cooling is deduced. The overall detection sensitivity, i.e. the number of molecules that need to be desorbed from the surface to be able to see one perylene ion in the detection region, is determined for perylene. The various factors that contribute to the overall detection sensitivity are discussed and, where possible, measured independently. In particular the ionization efficiency for jet-cooled perylene is measured independently. This enables us to give a molecule-independent apparatus constant for the overall detection efficiency.

### 1. Apparatus

A schematic of the experiment is shown in Fig. 1. The sample is mounted in front of a pulsed valve (General Valve) with a 0.5 mm nozzle diameter. The sample bar is positioned within 0.1 mm of the nozzle plate. The level of the sample can be varied continuously, and typically the sample is 0.5–2.0 mm below the molecular beam axis. The desorption laser hits the sample from above, and the position of the desorption laser spot relative to the nozzle can be adjusted. A telescope, providing a view along the desorption laser path, aids in the alignment. The desorp-

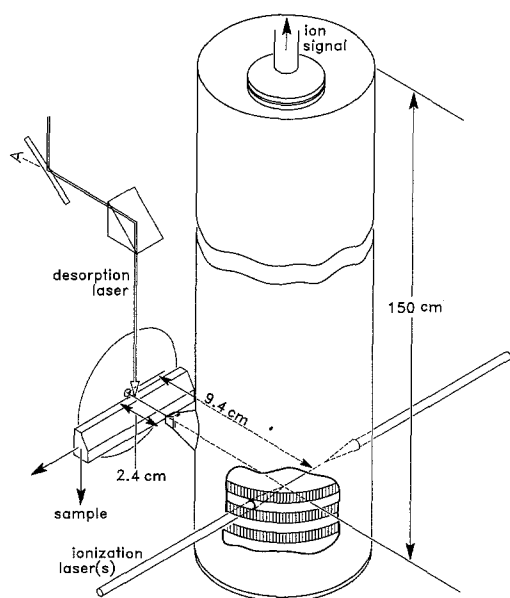


Fig. 1. Schematic view of the experiment. See text for details

tion laser spot has to be centered on the molecular beam axis. Positioning the spot 0.5–1.0 mm in front of the nozzle turns out to be best for optimum cooling. The sample is mounted on a rail, and a fresh part of the sample can be brought in front of the nozzle when needed. In all experiments described below, Ar, with a backing pressure of 8 atm, is used as the drive gas. The length of the gas pulse is 140–160  $\mu$ s. Timing of the desorption laser pulse with respect to this gas pulse is critical; best cooling and largest overall signal is obtained when the desorption laser is fired in a 20  $\mu$ s interval centered on the maximum of the gas pulse. Cooling and overall detection efficiency are much less when He is used as the drive gas. Results intermediate between those with Ar and He are obtained with CO<sub>2</sub> as carrier gas. Only the results with the Ar carrier are given. The experiment runs at a 10 Hz repetition rate.

Several types of sample holders are used, depending primarily on the vapor pressure of the molecules under study. In all cases the geometrical shape of the sample holder is as depicted in Fig. 1; the side of the holder away from the nozzle is bevelled off, to avoid disturbing the free jet expansion when the sample is close to the molecular beam. Desorption is performed from the 1 mm wide, flat top of the sample holder.

A major problem in the laser desorption jet-cooling technique is the shot-to-shot fluctuation in the amount of material injected in the jet. A small fluctuation in desorption laser power can cause a large fluctuation in the amount of desorbed material. When material is desorbed from a porous matrix the desorption laser power can be adjusted to completely remove the surface layer with each shot. The layer is replenished between desorption shots by diffusion from the bulk, and a more stable signal is obtained. This works especially well for molecules with a higher vapor pressure, which are more mobile in the matrix. Anthracene was dissolved in acetone and the solution put on fritted glass. The more volatile compound

diphenylamine was dissolved in methanol and put into activated carbon. Reasonably stable signals (shot-to-shot fluctuation less than 30%) were obtained in both cases. To determine the detection efficiency of the apparatus, calibrated layers of perylene on gold-coated copper were used as samples. Thin layers of perylene were vapor-deposited in vacuum, and the thickness of the growing layer was monitored by a quartz crystal balance. The calibration of the balance was checked by evaporating perylene on a quartz window and measuring its absorption in a UV photospectrometer. An extinction coefficient of  $\kappa = 3.8 \times 10^5 \text{ cm}^{-1}$  (at  $\lambda = 260 \text{ nm}$ ) was found, in perfect agreement with literature values [10]. Layers with a thickness down to 5 Å were made within 20% accuracy.

The optimum performance conditions for laser desorption jet-cooling from various sample substrates are remarkably similar. When changing sample substrates only the level of the sample with respect to the molecular beam axis and the desorption laser power need some minor adjustment.

A KrF (248 nm) excimer laser (Lumonics Hyperex-400; 15 ns pulse) is used for desorption. A 2 mm diameter spot is spatially cut out of the excimer beam profile, a few meters away from the laser. Calibrated attenuation filters are inserted in the resulting beam to reduce the intensity to 50–100  $\mu$ J. Then the beam is loosely focused by a 50 cm lens into a spot of less than 0.25 mm diameter on the sample. The size of the desorption laser spot on the sample is determined afterwards from the clearly observable holes in a homogeneous perylene layer as  $(4.3 \pm 0.2) \times 10^{-4} \text{ cm}^2$ . Both the size and the shape of the spot are reproducible within the indicated error margin.

Following desorption, the desorbed molecules are entrained in the jet and their internal degrees of freedom are cooled by multiple collisions with the drive gas. A fraction of the entrained molecules passes through the 1  $\times$  4 mm slit skimmer, 2.4 cm away from the nozzle. The beam enters the differentially pumped detection chamber, cooled to liquid nitrogen temperature, and is intersected, 9.4 cm away from the nozzle, by ionization laser(s). Ions are formed between the extraction plates of a Wiley-McLaren-type [11] linear time-of-flight mass spectrometer (R.M. Jordan Co.). The ions pass through a 150 cm long, grounded drift tube and are collected on a 2" dual channel plate. The signal from the channel plates is amplified 10 times by a fast, home-built pre-amplifier, before it is displayed on a digital oscilloscope (LeCroy 9400). The mass-spectra displayed on and stored in the scope are read out by an IBM PC. Under typical operating conditions, unit mass resolution up to 300 amu is obtained.

In order to determine the ion collection efficiency the transmission of the TOF was measured. The absolute number of positive ions produced between the extraction plates of the TOF was determined with a charge-sensitive amplifier, using the repeller plate of the TOF as an ion collector. This was compared with the absolute number of ions that reach the channel plates, by measuring the ion current on a stainless steel plate of the same size as and mounted in front of the channel plates. Acceleration voltages of 0–2 kV were used to collect the ions. In each

case a plateau was observed between complete collection and onset of secondary electron emission. The plateau charge was used to determine the ion number. For these experiments, laser-desorbed jet-cooled diphenylamine was used. Enough ions ( $\geq 10^4$ ) were produced per pulse to make detection with the charge-sensitive amplifier possible. An overall ion transmission of the TOF mass spectrometer of about 40% was found. It should be noted that the transmission of the TOF thus obtained is partly determined by the spatial distribution of the laser-desorbed jet-cooled diphenylamine in the beam, since the transmission through the TOF falls off rapidly with the distance from the TOF axis at which ions are created. As the spatial distribution will be similar for other laser-desorbed molecules, however, this is the relevant transmission.

The detection efficiency of the combined system of TOF, channel plates, pre-amplifier, and digital oscilloscope was calibrated by comparing the intensity of the parent peak in the mass-spectrum of diphenylamine, as displayed on the oscilloscope, to the absolute number of ions produced between the extraction plates, as measured with the charge sensitive amplifier. It was found that the number of ions produced between the extraction plates must be  $5/\sqrt{N_s}$ , to be able to detect a signal at the corresponding mass with  $\text{SNR} \geq 1$ , after averaging over  $N_s$  shots. To determine the presence of a certain ion in a single-shot experiment, at least five ions of this mass have to be produced in the detection region.

For resonant excitation of the jet-cooled organic molecules, the frequency-doubled output of a Quanta Ray or Lumonics dye laser pumped by the second and third harmonic, respectively, of a single Nd:YAG laser are used. For the ionization process either the same or the second dye-laser, an excimer laser, or the third harmonic of the Nd:YAG are used. An excimer laser, operating on KrF (248 nm), ArF (193 nm), or F<sub>2</sub> (157 nm), is also used for non-selective ionization of laser-desorbed species. All experiments are performed with unfocused ionization beams. The laser fluence applied for resonant excitation in the various organic molecules is on the order of 1–10  $\mu\text{J}/\text{mm}^2$ . For ionization out of the intermediate state laser fluences of 0.1–1.0  $\text{mJ}/\text{mm}^2$  are used.

The procedure for recording wavelength spectra is as follows: A mass spectrum is read out by the PC, and integration windows are set over several (maximum of five) mass intervals. The wavelength scan of the detection laser is controlled by the PC. At every wavelength setting a set of typically 10 mass spectra are recorded and averaged. Then the 10 Hz sequence is interrupted, the detection laser steps to its next wavelength, and the averaged ion signal in the various mass windows is calculated and displayed. The scan goes on over a pre-set wavelength interval, and at the end, wavelength spectra for the different masses are displayed. This final set of spectra is stored into memory. If needed, the difference of two wavelength spectra, or their ratio (for normalization purposes), is calculated and displayed.

## 2. Cooling Characteristics

### 2.1. Rotational Cooling

To determine the degree of rotational cooling, the rotational envelope of the origin of the  $S_1 \leftarrow S_0$  electronic transition of laser-desorbed anthracene was measured. The jet-cooled anthracene was pumped into its first electronically excited singlet state using the unfocused output of the frequency-doubled dye laser, operating on LDS 750 dye. Neutral density filters were placed in the beam to reduce the laser fluence to about  $2 \mu\text{J}/\text{mm}^2$  to avoid saturation of the resonant step. The lifetime of the vibrationless level in the electronically excited state is in the range 21–24 ns [12, 13]. Ionization out of the  $S_1$  state was performed with 307 nm radiation from another dye laser, thus reaching slightly above the ionization potential of 7.44 eV [14]. Ions were detected on the parent mass (178 amu). Since the energy of the  $S_1$  state in anthracene is less than half the ionization potential, the laser used for ionization out of this state can also perform two-photon ionization. This gives a constant ion background. Therefore, the intensity of the ionization laser was reduced so that on the peak of a strong resonance at least 95% of the ion signal is due to two color (1 + 1)-REMPI. In Fig. 2 the measured rotational contour of the  $S_1 \leftarrow S_0$  transition of

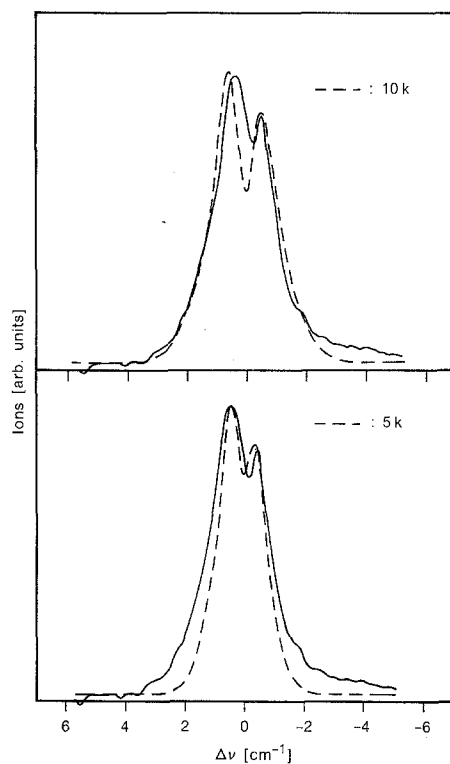


**Fig. 2.** Rotational envelope of the electronic origin of the  $S_1 \leftarrow S_0$  transition of laser-desorbed jet-cooled anthracene. The resonant excitation laser is scanned over the origin around 361.2 nm, and parent ions formed by ionization out of the  $S_1$  state using 307 nm radiation are detected. The experimental curve (solid line) is compared once with the simulated rotational contour assuming a 10 K rotational temperature (upper panel), and once with the rotational contour assuming a 5 K rotational temperature (lower panel). The simulated curves are convoluted with a  $0.5 \text{ cm}^{-1}$  laser linewidth [15]

anthracene (solid curve) is shown. The excitation laser was scanned in  $0.030 \text{ \AA}$  steps over the electronic origin at  $361.2 \text{ nm}$ . The ion signal at each wavelength position was averaged over 100 shots. The measured rotational contour is compared with the simulated rotational contour for a rotational temperature of  $10 \text{ K}$  (upper panel) and  $5 \text{ K}$  (lower panel). Simulated curves are taken from the work by Amirav et al. [15] and include a  $0.5 \text{ cm}^{-1}$  linewidth for the excitation laser, which is the same as the linewidth of our doubled dye laser. It should be noted that the frequency scale under the simulated contours in the work of Amirav et al. [15] has to be inverted, something they also noted themselves in comparing their experimental results with the calculations.

The rotational contour of the electronic origin shows the typical perpendicular (B-type) band shape, with a separated  $\Delta K = +1$  and  $\Delta K = -1$  branch, and a hole in the middle [15–17]. As explicitly noted in the work of Amirav et al. [15], there are three features in the rotational contour that are sensitive to the rotational temperature. Two of these, the frequency splitting between the  $\Delta K = +1$  and the  $\Delta K = -1$  branches and the depth of the minimum between them, are fitted best with the  $5 \text{ K}$  simulation. The third one, the overall width of the rotational contour, agrees best with the  $10 \text{ K}$  simulation. We conclude therefore that the rotational temperature of the laser-desorbed jet-cooled anthracene in our apparatus is between  $5 \text{ K}$  and  $10 \text{ K}$ .

## 2.2. Vibrational Cooling

To determine the degree of vibrational cooling, the fraction of vibrationally excited molecules in the electronic ground state was measured. Under normal operating conditions hot bands are not seen. When the sensitivity of detection is increased by several orders of magnitude, structure is sometimes recognized on the red side of the electronic origin. Care has to be taken to distinguish hot bands from lines of fragmented clusters of the molecules under study [5, 6]. The vibrational temperature was measured for diphenylamine laser-desorbed from activated carbon. Diphenylamine has low energy vibrational levels that are expected to be populated even at low temperatures. The spectrum is displayed in Fig. 3. It was recorded by detecting the parent ions ( $169 \text{ amu}$ ), after resonant  $S_1 \leftarrow S_0$  excitation followed by ionization at

$355 \text{ nm}$ . The laser fluence of the resonant excitation laser was about  $1 \mu\text{J}/\text{mm}^2$ . Several peaks indicated by an asterisk in the figure are due to diphenylamine-Ar complexes, most of which fall apart upon ionization and are detected on the diphenylamine mass. A detailed analysis of the diphenylamine spectrum and of the spectra of diphenylamine-Ar, Kr complexes will be given elsewhere [18]. Long progressions of low-frequency vibrations are seen in the vibronic spectrum, thus transitions to these levels have good Franck-Condon overlap. It is expected, therefore, that hot bands, starting from vibrationally excited levels in the electronic ground state, have appreciable transition strength as well. In the inset the region on the red side of the electronic origin is shown 100 times enlarged, and a hot band is recognized, shifted by  $-50.1 \text{ cm}^{-1}$ . This hot band is only observed when the delay of the detection lasers with respect to the desorption laser is such that an appreciable fraction of the molecules in interaction with the laser is warm (Sect. 3.4). The  $15 \text{ K}$  vibrational temperature deduced from the relative intensity of the hot band with respect to the electronic origin is therefore an upper limit for the vibrational temperature. It should be noted that vibrational cooling is expected to be efficient for diphenylamine due to its low energy vibrations. In all molecules studied, however, the fraction of vibrationally excited molecules in the electronic ground state was less than  $0.01$ .

## 3. Detection Sensitivity

### 3.1. General Considerations

The overall detection sensitivity of our laser desorption jet-cooling apparatus is one of the most important characteristics to be determined. One wants to know the minimum number of molecules,  $N_0$ , needed within the desorption laser spot on the surface in order to yield a detectable, mass- and wavelength-selected ion signal. The overall detection sensitivity  $P_0 = 1/N_0$  is molecule-dependent, but can be written as a product of the ionization efficiency  $P_i$  and the apparatus efficiency  $P_{\text{ap}}$  as  $P_0 = P_i \times P_{\text{ap}}$ .  $P_{\text{ap}}$  measures the probability with which the laser-desorbed molecules are brought into interaction with the detection laser(s), and is molecule-independent. The measurement of the overall detection sensitivity,  $P_0$ ,

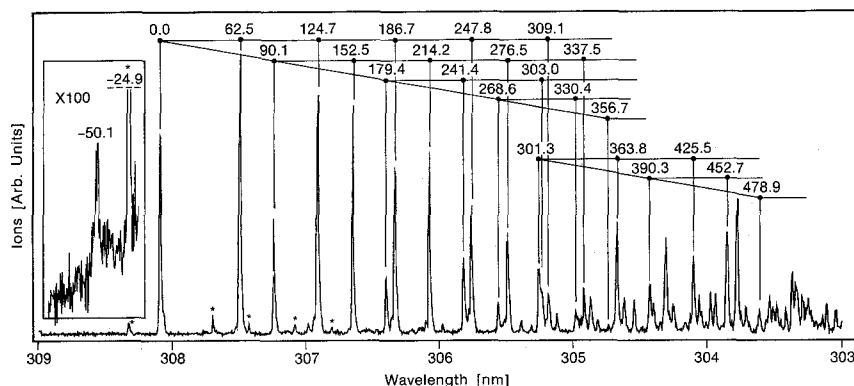


**Fig. 3.** Two-color (1+1)-REMPI spectrum of laser desorbed jet-cooled diphenylamine. Resonant excitation from  $S_1 \leftarrow S_0$  is performed using  $1 \mu\text{J}/\text{mm}^2$  of tunable dye-laser radiation between  $309\text{--}303 \text{ nm}$ , whereas ionization out of the intermediate state is performed with the tripled output of the Nd:YAG laser,  $355 \text{ nm}$ . Ions at the parent mass ( $169 \text{ amu}$ ) are detected. The lines indicated by an asterisk are due to the diphenylamine-Ar complex. In the inset, a weak hot band,  $50.1 \text{ cm}^{-1}$  redshifted from the electronic origin is recognized. From this a vibrational temperature of less than  $15 \text{ K}$  is deduced

for perylene is described in Sect. 3.2. In Sect. 3.3 an independent measurement to determine the ionization efficiency,  $P_i$ , for perylene is described. From these two measurements the apparatus efficiency  $P_{ap}$  is deduced, and the various contributions to  $P_{ap}$  are discussed in Sect. 3.4.

In selecting a molecule for performing sensitivity measurements, several factors were considered. To make a reliable sensitivity measurement, a molecule with a low vapor pressure at room temperature is needed. A small, well-defined amount of material must be put on the sample holder without being pumped off in  $10^{-6}$ – $10^{-7}$  Torr vacuum. To facilitate the independent measurement of the ionization efficiency, a molecule that can be efficiently ionized is preferred. Generally, a high ionization efficiency is possible for a molecule with the following characteristics: (i) The molecule has a resonant intermediate state at an energy more than half the ionization potential, so that the same laser can be used for resonant excitation and for ionization. In that case the perfect overlap of excitation and ionization laser, both spatially and temporally, favors a high ionization efficiency. (ii) The intermediate state has a lifetime at least as long as the pulse-length of the ionization laser. Otherwise the ionization out of this state will have to compete with other processes and might be less efficient. (iii) The molecule does not fragment upon ionization, even at high ionization laser fluences, as one wants the ion signal to be concentrated on a single mass peak.

We performed the sensitivity measurements on perylene, a molecule with a low enough vapor pressure, but with its first electronically excited singlet state at less than half the ionization potential. The lifetime of the vibrationless level in the  $S_1$  state is about 9 ns [19], long enough to make efficient ionization possible. Very often efficient and selective ionization is not possible simultaneously for molecules that need a higher frequency photon to be ionized from the intermediate state than the photon used for resonant excitation. The density of states above the first electronically excited state is often so high that most ions are produced by the ionization laser alone, by efficient two-photon ionization via this quasicontinuum, without any effect of the resonant excitation laser. Of course, one can reduce the intensity of the ionization laser to suppress the single color process relative to the resonant two-color (1 + 1)-REMPI process, but this reduces also the overall ionization efficiency. For perylene, however, it turns out that the 311.5 nm photon used for ionization from the  $S_1$  state produces hardly any ions by itself, even at the fairly high 0.5–1.0 mJ/mm<sup>2</sup> ionization laser fluence used. Laser desorbed, jet-cooled perylene was resonantly excited to the  $S_1$  state with 10 μJ/mm<sup>2</sup> of 416–400 nm radiation obtained via frequency doubling of the dye laser, operating on LDS 821 dye. After excitation with 415.8 nm light, at the electronic origin of the  $S_1 \leftarrow S_0$  transition, the onset for ionization out of the vibrationless level of the  $S_1$  state was found at 312.5 nm, in an electric field of approximately 290 V/cm. The field-free ionization potential is therefore around 6.96 eV, in perfect agreement with the value of 6.97 eV found for the adiabatic ionization potential via photo-electron spectroscopy [20].

Even at the highest ionization laser powers used, no fragmentation of the perylene was seen when the wavelength for ionization was chosen to just barely exceed the ionization limit.

### 3.2. Overall Detection Efficiency

Several measurements were performed to obtain reliable numbers for the overall detection efficiency of laser-desorbed jet-cooled perylene. Layers of 5, 20, and 50 Å of perylene were deposited on a gold-coated copper sample bar. The total number of ions formed in the detection region while depleting a desorption laser spot was measured. For these measurements the perylene was resonantly excited on the  $S_1 \leftarrow S_0$  0<sub>0</sub> transition, and subsequently ionized with 311.5 nm radiation. Both laser beams were confined to 1.2 mm diameter. The total perylene ion signal was measured with the channel plates. This signal was converted back to the actual number of ions produced between the extraction plates of the linear TOF using the channel plate and TOF calibration described in the apparatus section. To achieve total depletion of the desorption laser spot typically 200–1000 desorption laser shots were fired. A large fraction of the perylene is desorbed in approximately the first 20 shots. Later desorption laser shots desorb material from a somewhat larger area; an increase in the depleted area is seen with an increased number of shots. After the experiment, the actual desorption spot area was measured under a microscope. From this and from the film thickness the number of molecules originally in the desorption spot was determined.

For a measurement independent of the desorption spot size, a 1 mm<sup>2</sup> area of the sample was coated with 20 Å perylene, whereas the rest of the sample was uncoated. The sample was moved back and forth in front of the nozzle, until the whole area was depleted, and the total number of perylene ions measured.

All these measurements are in agreement with each other, yielding the result that  $(5 \pm 1)$  perylene-ions are formed in the detection region for every  $10^6$  perylene molecules originally in the desorption laser spot.

To demonstrate this sensitivity of the laser desorption jet-cooling technique a two-color (1 + 1)-REMPI spectrum of perylene using less than 30 picogram of material was recorded. For this a sample with a 5 Å perylene layer on top of a 600 Å coronene layer and covered with another 2000 Å coronene layer was used. The energy of the desorption laser thus was deposited in a thick layer of coronene rather than in the gold coating of the copper sample holder. This way the perylene came off the sample more equally distributed over the first 2000–3000 desorption shots. The resulting spectrum of perylene is shown in Fig. 4. It is important to note that the perylene spectrum was recorded without interference of the coronene, present in the beam in much larger amount. Ions were detected on the perylene mass while the resonant excitation laser was scanned over part of the  $S_1 \leftarrow S_0$  transition. The spectrum consists of 400 wavelength steps (0.16 Å each), and the signal was averaged over 6 shots at each wavelength setting. Apart from a strong origin, two

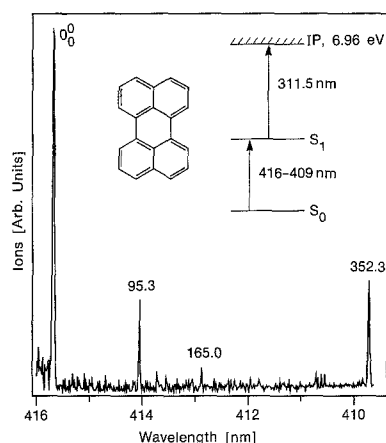


**Fig. 4.** Two-color (1+1)-REMPI of laser desorbed jet-cooled perylene. Only 30 picogram of perylene was originally in the laser spot. Resonant excitation from  $S_1 \leftarrow S_0$  is performed using  $10 \mu\text{J}/\text{mm}^2$  tunable radiation between 416–409 nm. Ionization is performed with  $0.5 \text{ mJ}/\text{mm}^2$  311.5 nm radiation. Ions at the parent mass (252 amu) are detected. The laser is scanned in  $0.16 \text{ \AA}$  steps, 400 in total, and the signal at every wavelength position is averaged over 6 shots

weaker vibrations at  $95.3 \text{ cm}^{-1}$  and at  $165.0 \text{ cm}^{-1}$  together with a strong vibration at  $352.3 \text{ cm}^{-1}$  are recognized. The spectrum is identical to the LIF spectrum of perylene [21]. As a low laser power was used for the resonant step, no overtones from the weaker vibrations are seen. The  $352.3 \text{ cm}^{-1}$  vibration should appear just as strong as the electronic origin. The difference in intensity indicates that the sample was partly depleted during the laser scan. From the thickness of the perylene layer together with the area of the desorption spot of  $(4.3 \pm 0.2) \times 10^{-4} \text{ cm}^2$ , we deduce that we started with 30 picogram of perylene in the desorption laser spot. At the end of the scan there is still some material left, and probably only 20 picogram was used. This means that on average 8.5 femtograms of perylene (33 attomoles) were desorbed per laser shot.

The signal to noise ratio in the spectrum of Fig. 4 is in agreement with the detection limits quoted before. 33 attomoles desorbed per laser pulse corresponds to about  $2 \times 10^7$  perylene molecules desorbed per pulse. From this we can produce  $(100 \pm 20)$  ions in the detection region, and by averaging over 6 desorption laser pulses a SNR of  $100/(5/\sqrt{6})$ , or approximately 50, is expected.

### 3.3. Ionization Efficiency

With the overall detection efficiency for perylene known, the ionization efficiency for jet-cooled perylene in our experiment must be determined to get the system parameter  $P_{\text{ap}}$ . This will allow us to predict the detection sensitivity for a specific molecule, once its ionization efficiency is known.

In Fig. 5a the experimental approach used to determine the ionization efficiency of perylene is shown. The sample used for this experiment was a  $2000 \text{ \AA}$  thick perylene layer on gold-coated copper, which gave a strong signal for a large number of desorption shots. In the detection region, between the extraction plates of the

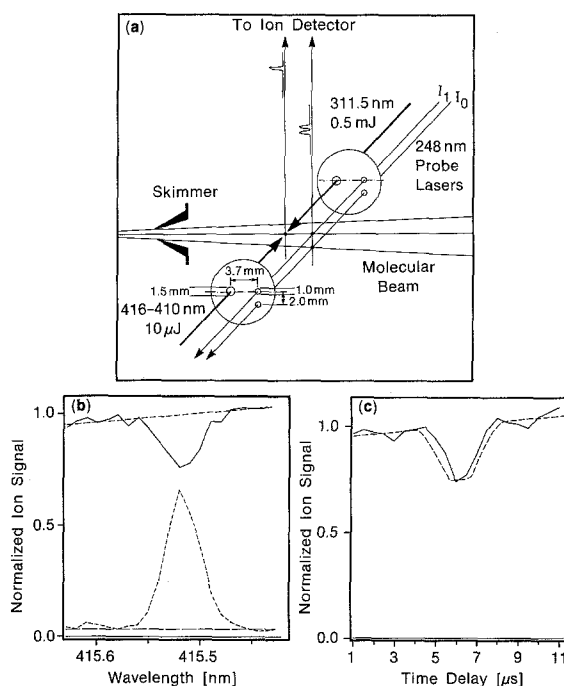


**Fig. 5.** a Experimental arrangement to measure the ionization efficiency of laser desorbed jet-cooled perylene. See text for details. b Ratio of perylene ion signal produced by probe beam  $I_1$  to that produced by probe beam  $I_0$  as a function of the wavelength of the laser used for resonant  $S_1 \leftarrow S_0$  excitation. A 25% depletion of the jet-cooled perylene in the beam is seen. The dashed curve in the lower part of the figure shows the simultaneously recorded two-color (1+1)-REMPI signal from the dye lasers, and demonstrates that the observed dip is exactly at the right wavelength. c With the dye laser used for resonant excitation fixed at the electronic origin of perylene, the ratio of the ion signal produced by either one of the probe beams is measured as a function of the time delay between the dye lasers and the probe laser. The dashed curve shows the simulated dip in the time dependence, assuming a homogeneous 25% depletion of the jet-cooled perylene over the 1.5 mm diameter area

TOF mass spectrometer, the molecular beam was intersected by four different laser beams. First it was intersected by the two different dye lasers, performing one-photon-resonant two-photon ionization, as described before. On both sides of the chamber a mask was placed to define the profile of the dye laser beams as a 1.5 mm diameter circle. Next, further downstream the molecular beam was probed by two spatially filtered beams out of the same excimer laser. The two beams were defined by 1.0 mm diameter apertures and were 2.0 mm above each other. Two-photon ionization of the perylene in the beam was performed by both excimer beams. The upper one was at exactly the same height as the dye lasers, and probed that part of the molecular beam which interacted with them. To probe the same time segment of the beam, a time delay of  $6 \mu\text{s}$  between the KrF and the dye lasers had to be used to enable the perylene molecules to travel the 3.7 mm distance. The combination of the two dye lasers and the upper of the two excimer lasers forms a typical pump-probe arrangement; depletion of the perylene in the beam performed by the dye lasers is probed by the excimer laser. The lower of the two excimer laser beams is used for internal calibration, needed because there is a large pulse-to-pulse fluctuation in the signal, as discussed before. The

upper of the excimer laser beams detects a small dip on top of a large, fluctuating background. This dip can only be recognized when the fluctuation is measured independently and simultaneously, and this is done by the lower of the excimer laser beams; it probes a part of the molecular beam that did not interact with the dye lasers. It does so in the same desorption laser pulse and with the same laser power with which the upper excimer laser beam probes the partly depleted region of the molecular beam. To separate the ion signal originating from either of the excimer laser beams, the voltage on the extraction plates is set far off the values needed to fulfill the Wiley-McLaren conditions; obviously space-focussing is not wanted in this case. Although this destroys the mass-resolution (the mass-peaks are much wider) it enables the probe laser signals to be clearly separated in time.

To determine the ionization efficiency, the ratio of the perylene ion signal produced by probe beam  $I_1$  to that produced by probe beam  $I_0$ , i.e. the normalized ion signal, was measured either as a function of the wavelength of the resonant excitation laser or as a function of the time delay between the dye lasers and the excimer laser. The solid curve in Fig. 5b shows the normalized ion signal when the resonant excitation laser was scanned over the  $S_1 \leftarrow S_0$   $0_0^0$  transition of perylene. A dip of almost 25% is seen. The dashed curve is the simultaneously measured two-color (1+1)-REMPI signal originating from the dye lasers, and is shown to demonstrate that the observed dip is indeed at the right wavelength position. In Fig. 5c the normalized ion signal is shown as a function of the time delay between the probe laser and the dye lasers. In this measurement the dye laser used for resonant excitation was kept fixed at the electronic origin of the perylene  $S_1 \leftarrow S_0$  transition. The maximum depletion occurred at a delay setting of 6  $\mu\text{s}$ , as mentioned before. The dashed curve shown in the same figure is the simulated time-dependence of the ion dip, assuming a homogeneous 25% depletion of all the perylene in the beam over the whole 1.5 mm diameter area. The width of the dip is narrower than that from the simulation. Thus efficient ionization takes place only in about 50% of the area defined by the masks.

These experiments indicate that a 25% ionization of all the perylene in the beam is achieved. The timing of the dye lasers was such that they only interacted with the coldest portion of the beam; see Sect. 3.4. Although the two-photon ionization with the KrF laser is expected to be equally efficient for cold and warm perylene molecules, at the time the dip is produced only cold molecules are present in the beam. Therefore we can conclude that the ionization efficiency is 25% for the cold perylene molecules in our beam. With 0.5 mJ of ionization laser power in an effectively 1.0 mm diameter spot, this means the cross-section for ionization out of the  $S_1$  state by 311.5 nm radiation, is about  $3 \times 10^{-18} \text{ cm}^2$ . This is under the assumption that the ionization step is not saturated. More likely, the ionization step is close to saturation, but the linewidth of the resonant excitation laser is narrower than the rotational envelope of the electronic origin, and only 25% of the ground state molecules are excited to the  $S_1$  state. Under this assumption an ionization cross-section of at least  $10^{-17} \text{ cm}^2$  is deduced.

The overall detection sensitivity for perylene, i.e. the fraction of perylene molecules originally in the desorption laser spot that produces an ion in the detection region, is found as  $P_0 = 5 \times 10^{-6}$ , see Sect. 3.2. The ionization efficiency  $P_1$  for the jet-cooled perylene is about 0.25, over the effectively 0.8 mm diameter area of the dye lasers. Therefore, more generally, our detection sensitivity for a given molecule is equal to  $2 \times 10^{-5}$  times the ionization efficiency of that specific molecule. The apparatus efficiency  $P_{\text{ap}} = 2 \times 10^{-5}$  consists of two factors: first, the fraction of laser-desorbed molecules which passes through the skimmer, and second, the fraction of molecules passed that interact with the detection laser.

### 3.4. Spatial Distribution of Entrained Material

In this section we discuss which fraction of the laser-desorbed molecules passes through the skimmer, and which fraction of those interacts with the detection laser. For this it is also necessary to discuss which portion of the entrained molecules is actually cooled. The spatial distribution of laser-desorbed jet-cooled diphenylamine was measured. The results obtained are typical for the spatial distribution of laser desorbed material in the Ar jet in our apparatus. In Fig. 6 the flight-time distribution of laser desorbed diphenylamine is shown. The horizontal axis shows the time-delay of the detection laser with respect to the desorption laser. The detection laser was kept at a fixed distance from the nozzle, 9.4 cm. The solid curve shows the time distribution of jet-cooled diphenylamine, that is, ions detected after one-color (1+1)-REMPI from the vibrationless level in the electronic ground state. The maximum signal was obtained when the detection laser was delayed 160  $\mu\text{s}$  with respect to the desorption laser, corresponding to a velocity of 587 m/s of the diphenylamine, only slightly higher than the 555 m/s velocity expected for a free Ar jet. The minor discrepancy might be explained by the nozzle being slightly above room

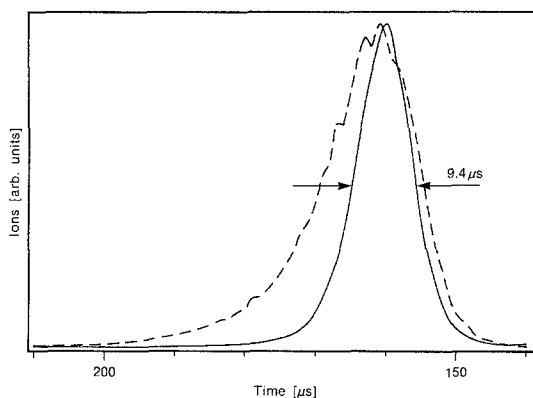


**Fig. 6.** Time distribution of laser desorbed diphenylamine arriving in the detection region, 94 mm away from the nozzle. One color (1+1)-MPI is performed, and parent ions (169 amu) are detected. The solid line is the time distribution of the cold diphenylamine molecules. The dashed line gives the time distribution of the total amount of laser desorbed diphenylamine. The curves are normalized to each other. The first part of the entrained cloud is effectively cooled, and the actual FWHM of the cold portion is about 5 mm



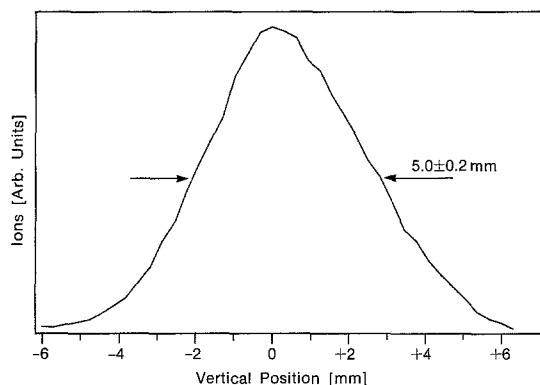


**Fig. 7.** Vertical distribution of laser desorbed yet-cooled diphenylamine in the detection region, at the time of maximum signal, 160  $\mu$ s after firing the desorption laser (Fig. 6). One-color (1 + 1)-REMPI with the laser at the electronic origin, is performed. A somewhat asymmetrical profile with a FWHM of 5.0 mm is seen

temperature (57° C) during constant operation. The FWHM of the jet-cooled diphenylamine is 9.4  $\mu$ s, corresponding to a horizontal distribution of 5.5 mm. It should be noted that a 1.0 mm diameter laser beam was used to record this distribution, and the actual spatial distribution of the jet-cooled diphenylamine was therefore somewhat narrower, closer to 5.0 mm. The dashed curve gives the flight time distribution of the total amount of diphenylamine coming through the skimmer, irrespective of their internal energy. This curve was obtained by two-photon ionization of the diphenylamine present in the jet using  $\lambda = 311$  nm, to the red side of the  $S_1 \leftarrow S_0$  transition. The latter curve is two orders of magnitude less intense than the solid curve, but in the figure the curves are shown normalized to each other. From (1 + 1)-REMPI spectra recorded at a time-delay of 160  $\mu$ s we know that at this delay the fraction of jet-cooled molecules is  $\geq 99\%$ . Normalization of the curves with respect to each other therefore shows directly that only those laser desorbed molecules that catch up with the Ar in the jet, those that show no velocity slip, are effectively cooled. The slower ones have higher internal energy. Only very broad and congested structure was observed when we tried to measure a (1 + 1)-REMPI spectrum of diphenylamine with the detection laser delayed by 170  $\mu$ s with respect to the desorption laser. From these results it can also be deduced that at least 50% of the total number of diphenylamine molecules coming through the skimmer was effectively cooled.

In Fig. 7 the vertical distribution of laser-desorbed jet-cooled diphenylamine is shown. The detection laser was delayed 160  $\mu$ s with respect to the ionization laser. A somewhat asymmetrical profile was observed when the 1.0 mm diameter laser beam was scanned from several mm below to several mm above the molecular beam axis. The FWHM of the vertical distribution was found to be close to 5.0 mm. This kind of distribution is expected from pure geometrical reasoning, the nozzle-to-skimmer distance being 1/4 of the distance from the nozzle to the detection region. Only minor differences in the vertical distribution profile were observed when the delay be-

tween the ionization and desorption laser was changed, or when ionization via the quasi-continuum was used for detection, thereby looking at all the diphenylamine molecules rather than only at the cold ones.

From these figures it is seen that typically 1.0–1.5% of the total number of laser desorbed molecules coming through the skimmer interacts with the detection lasers. This percentage is found by assuming an effective 0.8 mm diameter detection laser beam, as used in the measurement to determine the overall detection sensitivity for perylene. An improvement in detection sensitivity without a significant loss in mass resolution or in wavelength selectivity can be obtained by using a  $5 \times 1$  mm beam profile for the detection lasers, matched to the horizontal distribution of the jet-cooled material. Obviously, the detection sensitivity will only improve when increasing the detection laser area does not reduce the ionization efficiency by the same factor. This is most likely to be true when excimer lasers or YAG harmonics can be used for one-photon ionization from an intermediate, electronically excited state. For the resonant excitation step in the organic molecules studied, low laser fluences are sufficient and the excitation laser beam can simply be expanded and a  $5 \times 1$  mm portion cut out.

From the apparatus efficiency  $P_{ap} = 2 \times 10^{-5}$  and the 1.0–1.5% overlap of the laser-desorbed molecules that come through the skimmer with the detection laser, it is deduced that a fraction  $2 \times 10^{-3}$  of the laser-desorbed molecules is extracted through the skimmer. In an earlier publication in which the spatial distribution of laser-desorbed perylene in a He expansion was measured [9], an order of magnitude higher skimmer transmittance was estimated to be feasible. The experimental conditions are now optimized for both optimum cooling and optimum sensitivity and are different from the conditions applied then, which might well explain the discrepancy.

#### 4. Conclusions

We have experimentally demonstrated that a pulsed beam of rotationally (5–10 K) and vibrationally ( $\leq 15$  K) cold molecules can be produced with laser desorption jet-cooling. The overall detection sensitivity for perylene was found to be  $5 \times 10^{-6}$ , meaning that  $2 \times 10^5$  perylene molecules were needed in the desorption laser spot in order for one perylene ion to be produced in the detection region. Under the same conditions, the ionization efficiency for perylene was measured to be 25%. More generally therefore, our detection sensitivity for a given molecule is equal to  $2 \times 10^{-5}$  times the ionization efficiency of that specific molecule. The overall factor  $2 \times 10^{-5}$  contains a factor  $1 \times 10^{-2}$  for the spatial overlap of the jet-cooled molecules in the detection region with the detection laser, and a factor  $2 \times 10^{-3}$  for the fraction of laser desorbed molecules that actually comes through the skimmer. A two-color (1 + 1)-REMPI spectrum of less than 30 picogram perylene was recorded to demonstrate explicitly the high overall detection sensitivity that can be reached by laser desorption jet-cooling spectroscopy.



**References**

1. J.R. Cable, M.J. Tubergen, D.H. Levy: *J. Am. Chem. Soc.* **109**, 6198 (1987)
2. Liang Li, David M. Lubman: *Rev. Sci. Instrum.* **59**, 557 (1988)
3. J.R. Cable, M.J. Tubergen, D.H. Levy: *J. Am. Chem. Soc.* **110**, 7349 (1988)
4. *Lasers in Mass Spectrometry*, ed. by D. Lubman (Oxford University Press, Oxford 1990)
5. G. Meijer, M.S. de Vries, H.E. Hunziker, H.R. Wendt: *J. Chem. Phys.* **92**, 7625 (1990)
6. G. Meijer, M.S. de Vries, H.E. Hunziker, H.R. Wendt: *J. Phys. Chem.* **94**, 4394 (1990)
7. D.H. Levy: *Science* **214**, 263 (1981)
8. V.S. Letokhov: *Laser Photo-ionization Spectroscopy* (Academic, New York 1987)
9. P. Arrowsmith, M.S. de Vries, H.E. Hunziker, H.R. Wendt: *Appl. Phys. B* **46**, 165 (1988)
10. Y. Kamura, K. Seki, H. Inokuchi: *Chem. Phys. Lett.* **30**, 35 (1975)
11. W.C. Wiley, I.H. McLaren: *Rev. Sci. Instrum.* **26**, 1150 (1955)
12. J.S. Baskin, A.H. Zewail: *J. Phys. Chem.* **93**, 5701 (1989)
13. T.R. Hays, W. Henke, H.L. Selzle, E.W. Schlag: *Chem. Phys. Lett.* **77**, 19 (1981)
14. J.W. Hager, S.C. Wallace: *Anal. Chem.* **60**, 5 (1988)
15. A. Amirav, C. Horwitz, J. Jortner: *J. Chem. Phys.* **88**, 3092 (1988)
16. B.W. Keelan, A.H. Zewail: *J. Chem. Phys.* **82**, 3011 (1985)
17. W.R. Lambert, P.M. Felker, J.A. Syage, A.H. Zewail: *J. Chem. Phys.* **81**, 2195 (1984)
18. G. Meijer, M.S. de Vries, H.R. Wendt, H.E. Hunziker: To be published
19. A.J. Kaziska, S.A. Wittmeyer, A.L. Motyka, M.R. Topp: *Chem. Phys. Lett.* **154**, 199 (1989)
20. E. Clar, W. Schmidt: *Tetrahedron* **33**, 2093 (1977)
21. S. Leutwyler: *J. Chem. Phys.* **81**, 5480 (1984)